

# **CEOCOR**

**Comitè d'Etude de la Corrosion et de la Protection des  
Canalisations**

## **AC CORROSION ON CATHODICALLY PROTECTED PIPELINES**

**Guidelines for risk assessment and mitigation measures**

### **ANNEX N. 5 – 3**

**Influence of alkaline and earth alkaline Cations on the development  
of the spread resistance of cathodically protected coupons**

**F. Stalder**

## **5.3 Influence of alkaline and earth alkaline Cations on the development of the spread resistance of cathodically protected coupons**

### **5.3.1 Introduction**

In the context of investigations which the SGK conducted on AC corrosion incidences at the gas pipe-line in the Rhone valley the composition of the rust blister and of the circumvening soil were also investigated. It was found that in the vicinity virtually no lime is present in the soil. Apart from  $\alpha$ -FeOOH (goethite), larger quantities of sodium carbonate and sodium hydrogen carbonate were found within the rust blister. Furthermore substantial quantities of potassium carbonate and potassium sodium carbonate were detected. Further investigations showed substantial modifications of the spread resistance over time. Modifications up to a factor of 100 were observed. These modifications have been mentioned in investigations by various other authors. The investigations suggested that the soil composition at the fault locations and the area of the coupons are of significant influence. F. Stalder and D. Bindschedler established a hypothesis which was presented at the CEOCOR conference in Lugano. The hypothesis states that on fault locations in soils with a high lime content high resistivity covering layers develop which cause an increase of the spread resistance. In soils with low lime content however, a decrease of the spread resistance takes place due to the formation of hygroscopic alkaline hydroxides. This hypothesis had to be confirmed by further investigations.

Successively a project was set up which shall demonstrate, among other aspects, the influence of the soil composition on the spread resistance. Under laboratory conditions the influence of various  $\text{Na}^+$  and  $\text{Ca}^{2+}$  ion contents shall be shown by means of artificial soil solutions.

### **5.3.2. Implementation of the laboratory experiments**

#### **5.3.2.1. Set-up**

Cylindrical probes consisting of non alloy steel were molded in insulating plastic material. The circular exposed surface area measured  $1 \text{ cm}^2$ . In fig. 5.3.1 the experiment probe is sketched.

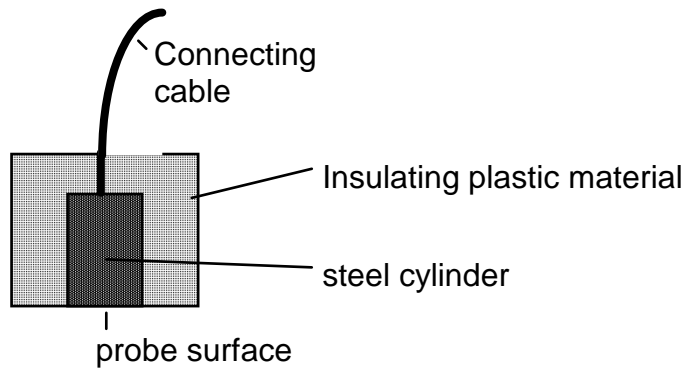


**Fig. 5.3.1: Coupons used for the experiments**

The probes were embedded in boxes filled with quartz sand (see fig. 5.3.2). Prior to putting them into place the probes were wet ground by means of 320 grid SiC grinding paper and cleaned in an ethanol ultrasonic bath. Embedding the probes in sand results in similar diffusion environments as present in natural soils. Without sand any reaction products formed would be transported away from the surface too rapidly. By using pure quartz sand it is guaranteed that no undesirable contaminations are inserted. The grain size of the applied sand was of 0.3 – 0.9 mm. A stainless steel counter electrode (anode) is placed at the bottom of the boxes. From a reservoir placed above, artificial soil solution can be dispensed to the sand filled basin in well controlled doses. Two drain openings at different elevations on the basin allow a variation of the water level in the basin. By means of these, experiments may be performed which simulate the position of the probe above and below the artificial ground water level.

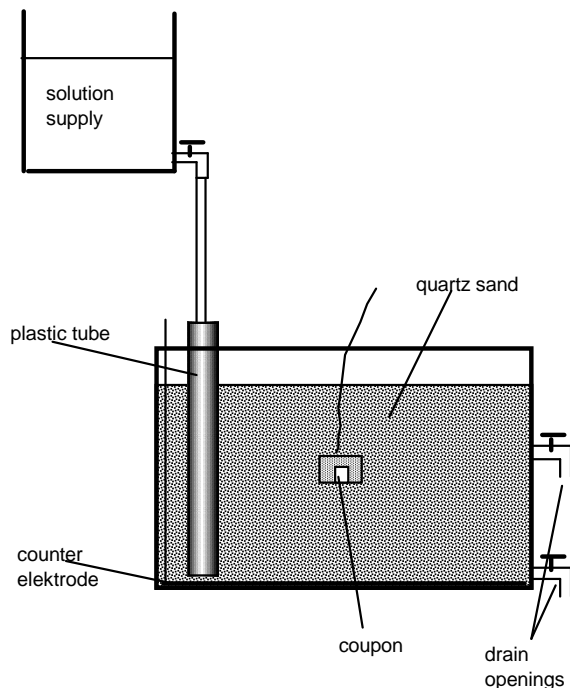


**Fig. 5.3.2.: Setup for measuring the spread resistance**

### 5.3.2.2. Implementation

The measurements were carried out with different concentrations and  $\text{Na}^+$  to  $\text{Ca}^{2+}$  ion ratios. The requested concentration was achieved by adding  $\text{NaNO}_3$  and  $\text{Ca}(\text{NO}_3)_2$ . The solutions used are listed in table 5.3.1. The addition rate of the solution was set to approx. 1l per 24 hours. Per series five experiments were conducted in parallel. In the A and B test series deionized water was used, for the C series, tap water of the city of Zurich with a total hardness of 1.65 mmol was used. In series A and C, the measuring probes were situated below the artificial ground water level, in series B above.

		Test 1	Test 2	Test 3	Test 4	Test 5
Series A / B	Na:Ca mol ratio	0:1	1:2	2:1	8:1	1:0
	Conductivity [ $\mu\text{S}$ ]	595	621	589	596	605
Series C	Na:Ca mol ratio	0.3:1	1:2	1.1:1	3.7:1	8.8:1
	Conductivity [ $\mu\text{S}$ ]	559	571	575	571	574

**Table 5.3.1.: Survey over applied solutions**

The probes were protected cathodically. The DC rectifier voltage was set to approx. 2V at the beginning. The off potential therefore was  $-1050 \text{ mV}_{\text{SCE}}$ .

The test period was approx. 30 days. During this time the off potential, the resistance between counter electrode and probe, as well as the protective current were recorded. The resistance was measured by means of an AC resistance meter at a frequency of 1 kHz. The value obtained in this manner corresponds approximately to the spread resistance of the probe. The potential and current measurements were conducted by means of a Fluke 87 multimeter.

### 5.3.3. Results, Evolution of the Spread Resistance

The evolution of the spread resistance (resistance coupon – counter electrode) for the A and B series is displayed in fig. 5.3.3. and 5.3.4. The resistance of the measuring probe in a solution with a  $\text{Na}^+ / \text{Ca}^{2+}$  ratio of 0 : 1 is increasing significantly over time, whereas the resistance of the probes in a solution with a  $\text{Na}^+ / \text{Ca}^{2+}$  ratio of 1 : 0 is decreasing. Differences between the individual probes become more distinct after a test period of approx. 20 days. The resistance modification of the remaining probes is less significant. However, probes in a solution with a higher  $\text{Ca}^{2+}$  content show a tendency towards a higher resistance value. When the same measurement is performed with probes above the artificial ground water level the recorded changes occur significantly more slowly. The probe with  $\text{Na}^+$  -cations only equally shows the lowest resistance of this series. For the remaining probes, in solutions with  $\text{Ca}^{2+}$  ions, no clear distinction of the development over time is possible. Fig. 5.3.5. displays the evolution of the spread resistance of probes in solutions prepared out of tap water. Here modifications of the measured values over time can hardly be detected.

Upon termination of the experiment the measuring probes were removed, rinsed with water and examined visually. Photographs of the probes are displayed in appendix 1. Probes exposed to solutions with higher calcium content show significantly more sand grains sticking firmly to the surface. Probes in solutions without calcium ions no sand grains adhere to the surface. Special attention is attracted to the fact that the

noticeable visual differences of the B and C series are larger than one would expect from the registered measuring values.

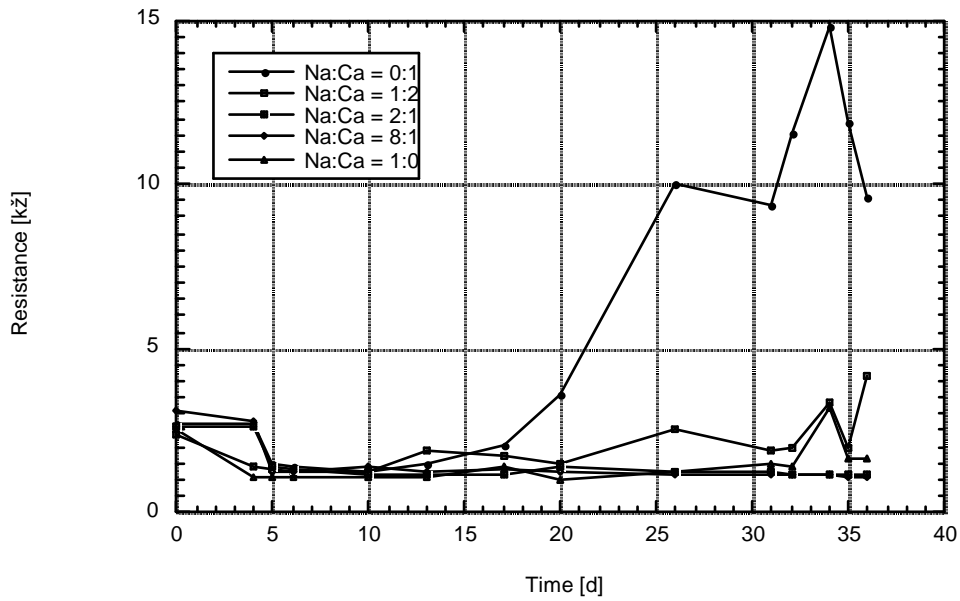


**Fig. 5.3.3: Evolution of the spread resistance of coupons below the ground water level (A series)**

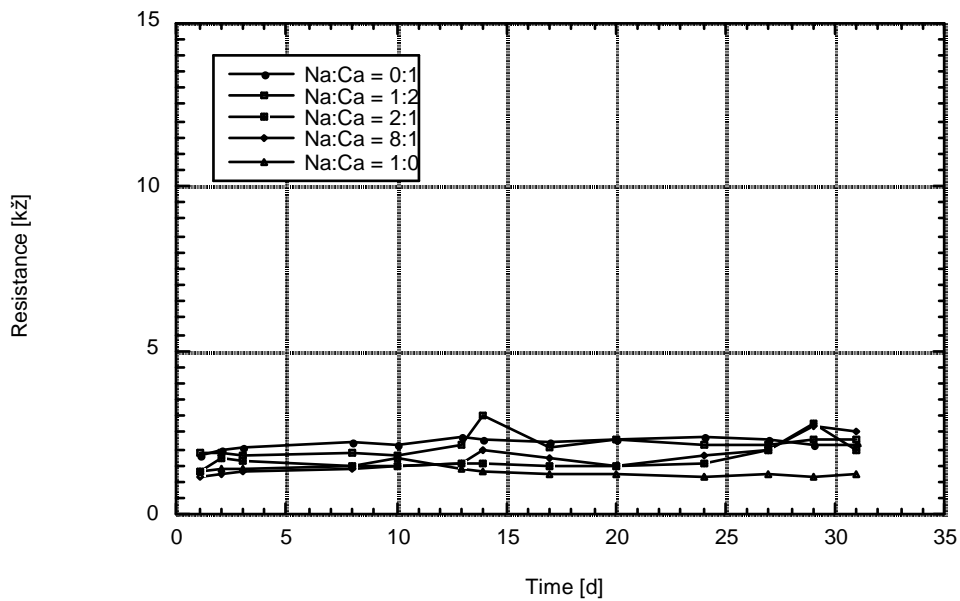


**Fig. 5.3.4: Evolution of the spread resistance of coupons above ground water level (B series)**

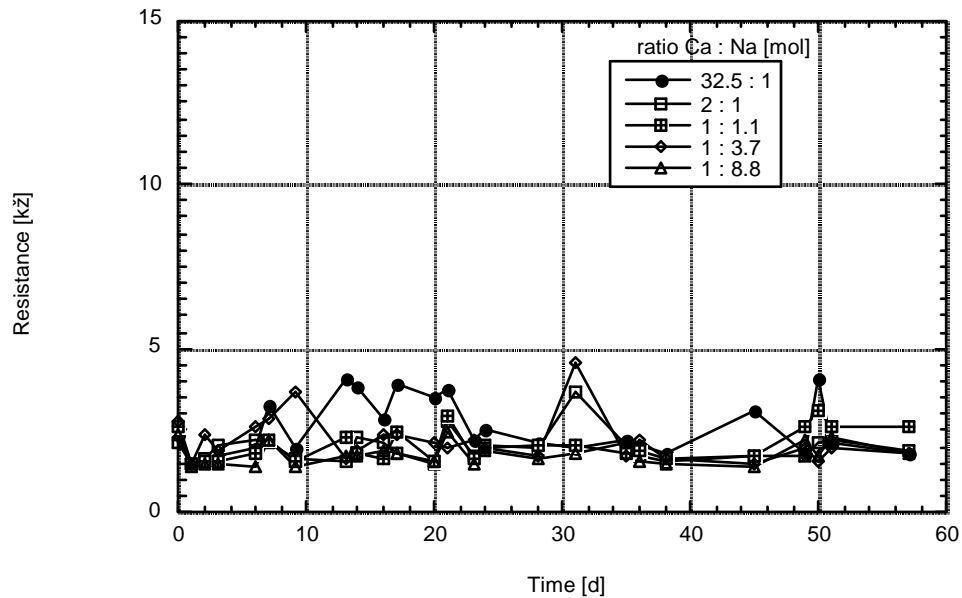


**Fig. 5.3.5: Evolution of the spread resistance of coupons below ground water level in solutions prepared with tap water (C series)**

### 5.3.4. Discussion

The results of the experiments (measured values and visual inspection) in artificial soil solutions demonstrate an influence of the composition on the spread resistance. The hypothesis formulated by F. Stalder and D. Bindschedler seems to be confirmed.

According to this hypothesis, in soils rich in  $\text{Na}^+$  ions, but having no  $\text{Ca}^{2+}$ , the  $\text{OH}^-$  formed at the probe surface by the cathodic protection is transformed into  $\text{NaOH}$ . The latter can further react with  $\text{CO}_2$  present in the soil into sodium carbonate and sodium hydrogen carbonate. Sodium carbonate and sodium hydroxide are well soluble in water and furthermore, they are hygroscopic, i.e. they attract water. These substances accumulate in the region of the fault location (coupons) and increase the conductivity. The spread resistance decreases. In soil solutions rich in lime, the  $\text{Ca}^{2+}$  ion, together with  $\text{OH}^-$ , is transformed into  $\text{Ca}(\text{OH})_2$ . The latter may further react with  $\text{CO}_2$  into  $\text{CaCO}_3$ , and, in a further step into  $\text{Ca}(\text{HCO}_3)_2$ . These reaction products, particularly  $\text{CaCO}_3$ , have low solubility. This leads to precipitations, i.e. formation of covering layers at the probe surface. This phenomenon could be observed in the experiments. The higher the share of  $\text{Ca}^{2+}$ , the more sand grains are glued at the probe surface, since more lime is formed. The spread resistance increases. When  $\text{Na}^+$  and  $\text{Ca}^{2+}$  ions are present in comparable quantities, the two reactions compete with each other. Covering layers build up, but simultaneously the conductivity in front of the measuring probe increases. The modifications of the spread resistance are smaller.

In the experiments where the measuring probe is situated above the artificial ground water level the modification of the spread resistance develops significantly more slowly. This can be related to the fact that the ion transport mechanism takes place only in a comparably thin humidity film at the surface of the sand grains. In the solutions prepared with Zurich tap water no clear modifications can be detected. This

in turn attributes to several coincident reactions. Nevertheless, the visual inspection showed that also under these conditions a lime layer is formed. As a tendency it can be concluded that the higher the  $\text{Ca}^{2+}$  ion content the more evident the effect.

Fig. 5.3.6. displays a model concept describing the regions in front of a fault location (measuring probe) wherein reactions may take place, and the distribution of the pH value. It is based on a protecting current of  $2 \text{ A/m}^2$ . The fault location area is  $1 \text{ cm}^2$ .

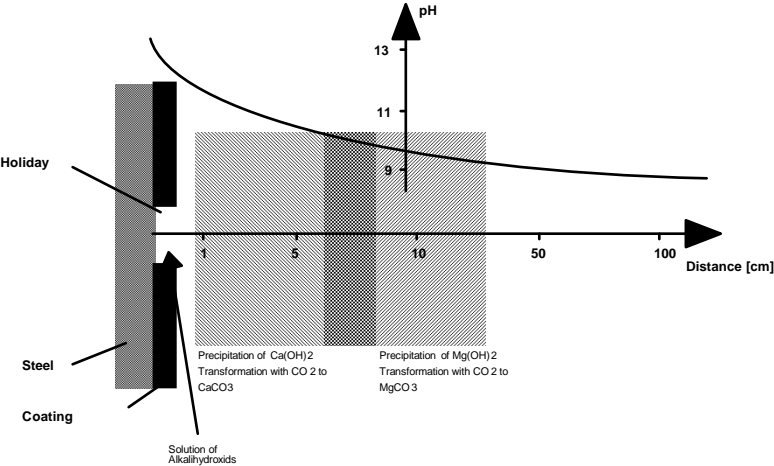


**Fig. 5.3.6: Conceptual model of the pH value distribution and possible reaction regions at a fault location**